CHAPTER IV
RESULTS AND DISCUSSION

According to the previous work on these same gold surfaces treated identically as was done in this study (Gutig *et al.*, 2008) the gold surface was not hydrophobic; as reported previously the contact angle was 10 ± 2° and XPS measurements that showed that the oxygen content of the surface was 36.3% compared to gold at 26.6%. In addition, the actual surface area of gold using AFM was estimated at 1.39 cm^2, compared to the nominal surface area of 0.79 cm^2.

4.1 CMC Determination

Critical micelle concentrations (CMC) of AOT and Tween 20 as measured by surface tension are shown in Table 4.1 compared to literature data. As shown in Table 4.1, acceptable agreements was achieved. Regarding AOT, the difference between literature data might be due to impurities in the samples. While Fragneto *et al.* (1996) purified AOT by liquid-liquid extraction, and found a CMC of 2.50 mM, Grillo and Penfold (2011) measured the CMC of AOT (purity > 98%) without additional purification, and found that the CMC was 3.13 mM. As mentioned in the Methods section, the surfactants were used as received.

Table 4.1 Critical Micelle Concentrations of AOT and Tween 20

	CMC (mM)	
	Current Study	**Previous Measurements**
AOT	2.91 ± 0.12	2.50 (Fragneto *et al.*, 1996), 3.13 (Grillo and Penfold, 2011)
Tween 20	0.08 ± 0.002	0.06 (Mahmood and Al-Koofee, 2013)

4.2 Adsorption Isotherms

4.2.1 Adsorption of AOT

The adsorption isotherm for AOT at 25 ± 0.05°C, calculated using the Sauerbrey relation, is shown in Figure 4.1 (black circles). The isotherm follows the typical L2 features (Giles *et al.*, 1974). The amount of AOT adsorbed per unit of surface area increases continuously on gold surface up to the bulk concentration of 1.7(CMC) and then reaches a plateau. The surface density of AOT in correspondence of a plateau in terms of mass and mole adsorption is reported in Table 4.2. It would have been expected that the adsorbed mass does not increase above the CMC, although some papers report an increase in mass adsorbed above the CMC. For example, Esumi *et al.* (2001) found an increase in adsorption above the CMC for $C_{10}E_6$ on silica, and suggested that the hydrogen bonds between the ether oxygen atoms of the surfactant and the hydroxyl groups of silica, plus the intermolecular hydrophobic interactions were two factors driving this behavior. Specifically, at low concentrations the authors postulated that $C_{10}E_6$ lies flat on silica and, as the concentration increases, surfactant tails tend to be squeezed out and become perpendicular to the surface to form a closely packed adsorbed layer. The authors suggest that this transformation does not conclude until the concentration is higher than the CMC. Lippold and Quitzsch (2000) found that the adsorption of the nonionic surfactant decanoyl-N-methylglucamide (MEGA-10) on silica gel increased above its CMC. These authors postulated an increase in the amount of non-associated monomers in the bulk above the CMC, which in turn increased the adsorbed amount. In this case, since the amount of surface area relative to the mass of surfactant is quite low and AOT was used without additional purification, the adsorption isotherm might be affected by impurities such as monoester, diester, ethylhexanol, and residues from the manufacturing process. As micelles form, some of the co-adsorbed minor component could partition to the micelles, which in turn affects the amount adsorbed at the solid interface; such effects are well-known in surface tension measurements. In a previous publication (Wu *et al.*, 2011), they attributed an anomalous feature in the adsorption isotherm (a large peak in adsorption at the CMC) to impurities.

QCM-D also measures the change in dissipation, which is related to the viscoelastic properties of the surface aggregates. This measurement enables the assessment of flexibility of the adsorbed layer. In Figure 4.2, the dissipation is shown for AOT as a function of bulk concentration (black circles). The change in dissipation remains below 2 x 10^{-6} within the entire range of concentrations considered, indicating that the AOT film is not very viscoelastic (Vogt *et al.*, 2004). However, the dissipation increases with concentration, especially near to and above the CMC. Some researchers have previously suggested that morphology affects dissipation (Shi *et al.*, 2009). Specifically, they observed a decrease in the measured dissipation, which they attributed to a change in adsorbed CTAB aggregate morphology from cylindrical to flat bilayer structure.

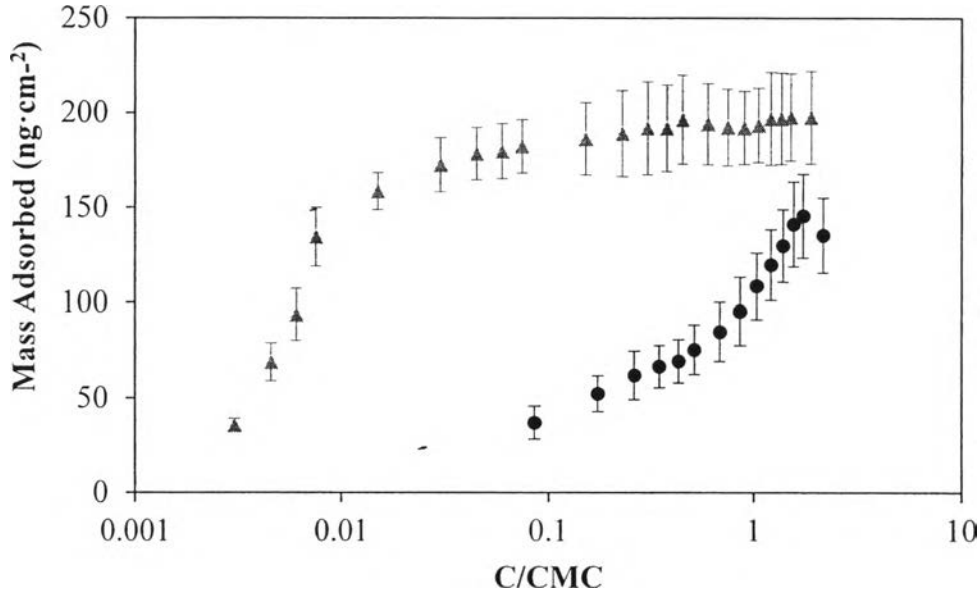

Figure 4.1 Experimental adsorption isotherms for AOT (●) and Tween 20 (▲) measured on a gold surface at 25 ± 0.05 °C as a function of bulk concentration. The adsorbed amount is estimated using the Sauerbrey relation. The bulk surfactant concentration is normalized by the CMC of each respective surfactant (see Table 4.1).

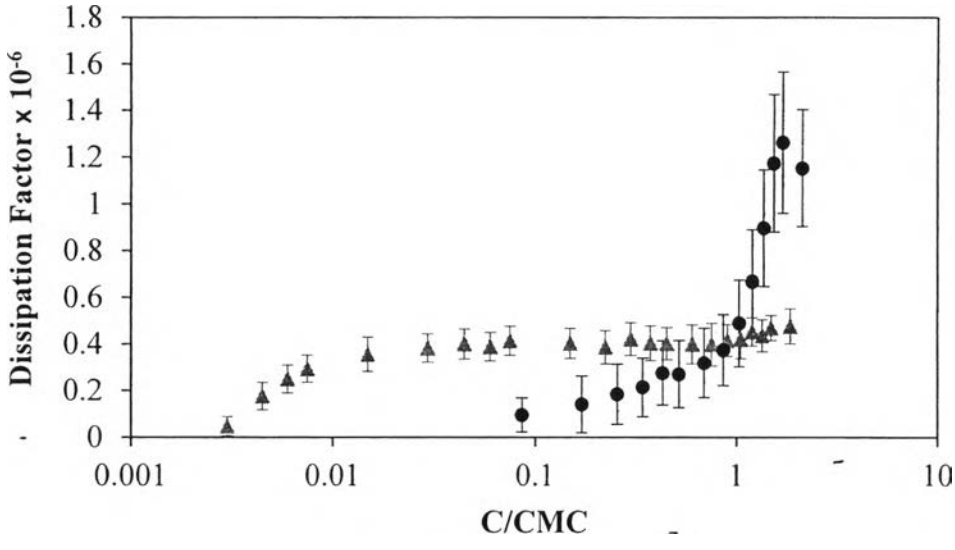

Figure 4.2 Measured change in energy dissipation for AOT (●) and Tween 20 (▲) measured on a gold surface at 25 ± 0.05 °C as a function of bulk concentration. The data correspond to the adsorption isotherms shown in Figure 4.1.

Table 4.2 Surface Adsorption Density of AOT and Tween 20 on Gold above the CMC

	Adsorbed mass ($ng \cdot cm^{-2}$)	Adsorbed mole (10^{-12} $mol \cdot cm^{-2}$)
AOT	146 ± 22	328 ± 28
Tween 20	197 ± 23	160 ± 10

Although the dissipation is less than 2×10^{-6} in the entire adsorption isotherm, and hence the Sauerbrey relation should hold, the raw AOT adsorption data were also fitted to the Voigt model, using the Q-tool software, to check that the presented adsorbed mass values did not depend substantially on the model chosen. AOT data were selected to fit to the Voigt model rather than Tween 20 since the dissipation of AOT is higher than Tween 20 (see Figure 4.2). To implement the Voigt model it is necessary to assume values for the density of the adsorbed layer, the density of the supernatant, and the viscosity of the supernatant. These were assumed to be 1,050 $kg \cdot cm^{-3}$, 1,000 $kg \cdot cm^{-3}$, and 0.001 $kg \cdot m^{-1} \cdot s^{-1}$, respectively. The

mass adsorbed calculated by Voigt model (grey circles) are compared with the Sauerbrey relation (black circles) in Figure 4.3. Clearly, the two models do not differ within the experimental accuracy of the data. All data presented in this work, except that in Figure 4.3, were obtained using the Sauerbrey relation.

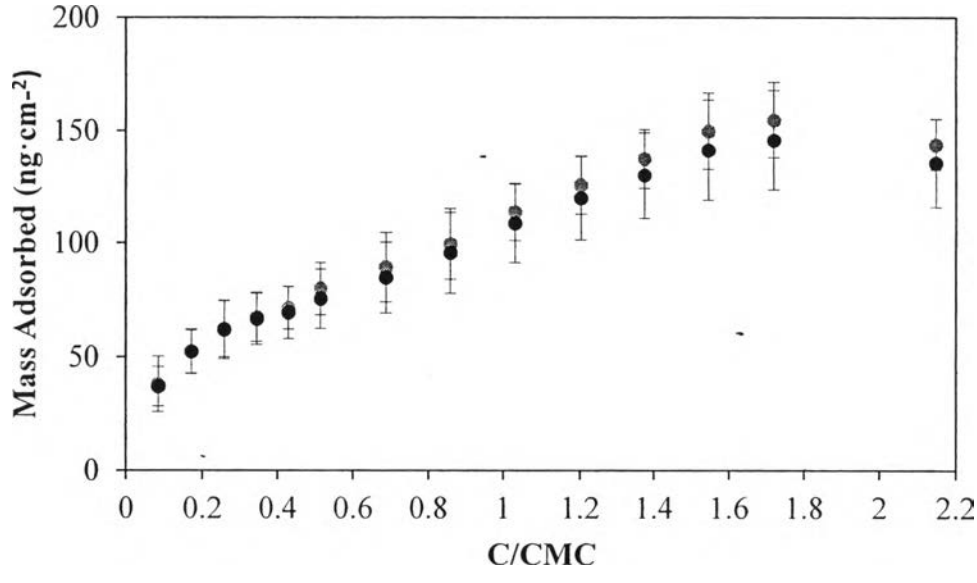

Figure 4.3 Experimental adsorption isotherm for AOT on gold at 25 ± 0.05 °C calculated by both the Sauerbrey relation (●) and the Voigt model (●).

4.2.2 Adsorption of Tween 20

The adsorption isotherm for Tween 20 is shown in Figure 4.1. Also this isotherm reproduces the typical L2 features (Giles *et al.*, 1974). The maximum amount adsorbed is higher for Tween 20 than for AOT indicating that packing is more efficient for Tween 20. Efficiency is defined as atoms adsorbed per unit surface area. Amounts adsorbed for Tween 20 above its respective CMCs are reported in Table 4.2.

Tween 20 is found to partition heavily on the surface even at low bulk concentrations. In fact, adsorption is complete already at about 0.15(CMC). Similar observations were reported by Martín-Rodríguez *et al.* (1997), who studied the adsorption of Tween 20 onto latexes. They found that the amount of Tween 20 adsorbed reached a saturation value at about 0.3(CMC). The dissipation measured

for adsorbed Tween 20 aggregates is shown in Figure 4.2 (grey triangles). The low dissipation indicates a rigid film; the value of 0.4 x 10^{-6} for Tween 20 is lower than that for AOT and also lower than that reported previously for CTAB (Gutig *et al.*, 2008; Shi *et al.*, 2009). Lower dissipation was not expected, given the molecular architecture of Tween 20. However, Tween 20 has been shown to adsorb more strongly than Tween 40 on hydrophobic gold even though Tween 40 has a longer hydrophobic tail than Tween 20 (Shen *et al.*, 2011). Based on the fit of adsorption models for Tween 20 vs. Tween 40, the authors postulated that for Tween 20 when the surface coverage was low, the surfactant adsorbed by hydrophobic interaction with the surface and the tail group laid essentially flat on the surface. Once the surface coverage became high, Tween 20 could self-organize itself to allow other molecules to adsorb on the surface and form a high-density layer with cooperative interactions between Tween 20 molecules. For Tween 40, a simpler single mechanism adsorption was found adequate to fit the adsorption data (Shen *et al.*, 2011).

4.2.3 Adsorption of AOT on a Crystal Covered by an Adsorbed Tween 20 Film

A film of Tween 20 on gold was prepared (details in the Methods section), and then exposed this film at increasing concentrations of aqueous AOT at 25 ± 0.05 °C. The results are shown in Figure 4.4. A small decrease in the mass adsorbed occurred when 0.1(CMC) of AOT was added, suggesting that some Tween 20 was removed from the surface. As the AOT concentration increased from 0.1(CMC) to 1.0(CMC), both the adsorbed amount and the dissipation did not change, indicating that either (1) AOT displaces exactly the same amount of Tween 20, or (2) AOT does not displace additional Tween 20. With the differences in molecular properties (Mw, architecture, ionic features, etc., Figure 3.1), between the two surfactants, it is likely that no displacement of Tween 20 by AOT occurred. When the AOT concentration is increased above its CMC, the amount adsorbed increased. It is interesting to point out that the mass adsorbed at the highest AOT concentration considered in Figure 4.4 corresponds to the mass of Tween 20 adsorbed when no AOT was present in the system. Comparing the adsorption data

for AOT alone and for AOT in the presence of a pre-adsorbed Tween 20 film, the data suggest that the film obtained adding AOT to the pre-adsorbed Tween 20 film has larger mass than that obtained using only AOT. This additional adsorption seems to happen above the AOT CMC, and it might be due to partition of impurities to the adsorbed film. Overall, the results indicate that the final film is composed of both AOT and Tween 20. Unfortunately, QCM data are not sufficient to separate the two components. Other measurements can quantify surface coverage of each component; Thibaut *et al.* (2000) observed the adsorption of the anionic surfactant SDS on silica precoated with the nonionic surfactant $C_{10}E_5$. They found $C_{10}E_5$ desorbed and formed mixed micelles with SDS; the latter was determined via free energy calculations. Moreover, they observed an enthalpy increase when SDS was added due to the heat of mixing between desorbed $C_{10}E_5$ and the SDS due to mixed micelle formation.

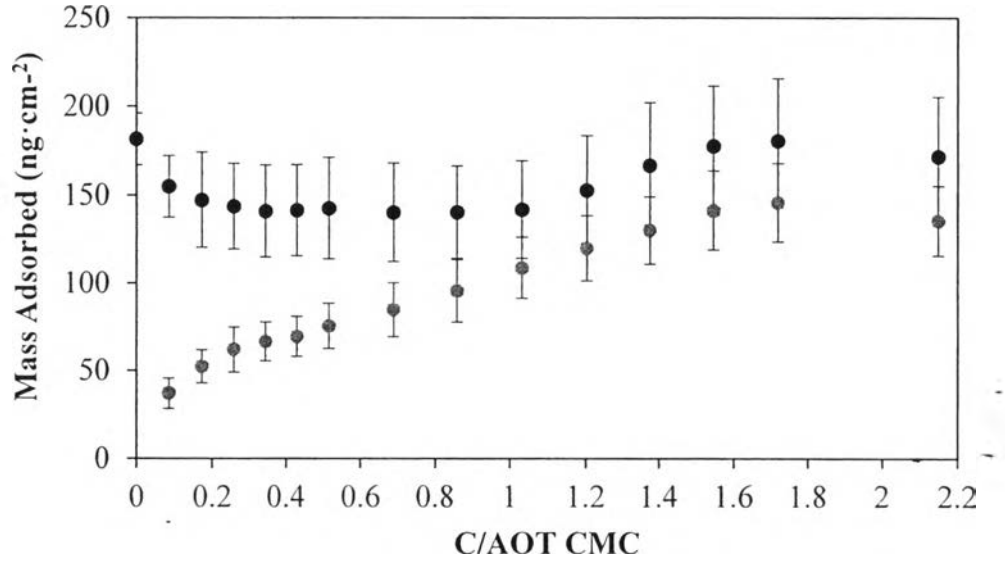

Figure 4.4 Experimental adsorption data as a function of bulk concentration at 25 ± 0.05 °C obtained when an aqueous system containing AOT (at increasing concentration) and Tween 20 (at 1.4 Tween 20 CMC) was flown over a gold surface covered by a pre-formed Tween 20 film (●). The results are compared to the adsorption isotherm obtained for AOT (●), data reproduced from Figure 4.1.

The dissipation data are shown in Figure 4.5. When AOT is added to a Tween 20 film, the dissipation scales with adsorbed amount in all three regions: from 0 to 0.1(CMC), from 0.1(CMC) to 1.0(CMC) and above 1.0(CMC). Specifically, a drop occurs in dissipation from 0 to 0.1(CMC), although the ΔD drop may not be outside of experimental error. From 0.1(CMC) to 1.0(CMC), the dissipation remains constant and the value of 0.4×10^{-6} is the same as pure Tween 20 dissipation (see Figure 4.2). Above the AOT CMC, the dissipation is lower than that of pure AOT, but it increases to values larger than those reported for Tween 20. Hence, both measurements clearly indicate that the surface coverage is a mixture of Tween 20 and AOT when Tween 20 is pre-adsorbed and AOT is added.

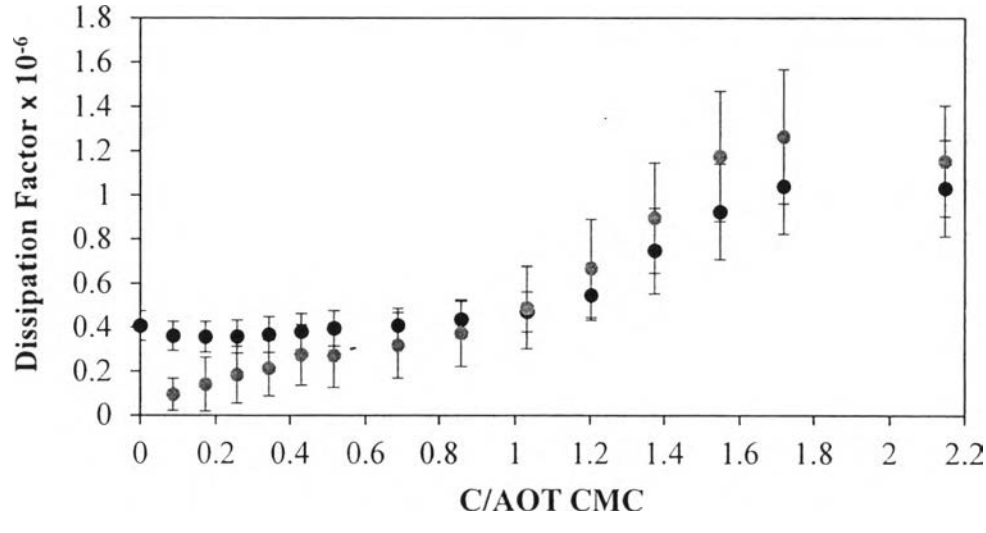

Figure 4.5 Measured energy dissipation for AOT (●) and AOT precovered with Tween 20 (●) on gold surface as a function of bulk concentration corresponding to the adsorption isotherm in Figure 4.4. The results are compared to the dissipation obtained for AOT (●), data reproduced from Figure 4.2.

4.2.4 Adsorption of Tween 20 on a Crystal Covered by an Adsorbed AOT Film

The experiments of Figures 4.4 and 4.5 were repeated, but preparing an AOT film and then increasing gradually the Tween 20 concentration. Adsorption

isotherms and dissipation are shown in Figures 4.6 and 4.7, respectively. When Tween 20 is added to the system, the results show that the adsorbed mass increases (unlike the results discussed in Figure 4.4). The amount adsorbed increases quickly at Tween 20 concentrations lower than ~ 0.5 its CMC, then a little slower up to Tween 20 concentrations below ~ 1.4(CMC), at which point a plateau is reached. The continuously increase in adsorbed mass of Tween 20 to the AOT film is due to the fact that the nonionic surfactant can reduce the electrostatic repulsion between headgroups of the anionic surfactant so that more surfactants can adsorb on the surface (Somasundaran *et al.*, 1992). The adsorbed mass correspondent to this plateau is similar, within experimental uncertainties, to that of pure Tween 20 adsorbed on gold above its CMC. This result is similar to that discussed in Figure 4.4 when the two surfactants were added with reversed order.

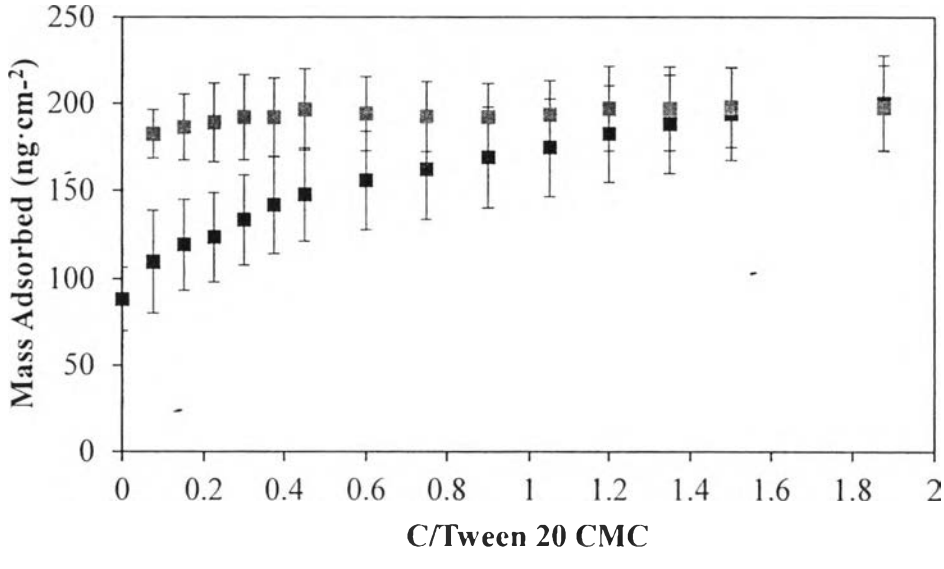

Figure 4.6 Experimental adsorption data as a function of bulk concentration at 25 ± 0.05 °C obtained when an aqueous system containing Tween 20 (at increasing concentration) and AOT (at 1.4 AOT CMC) was flown over a gold surface covered by a pre-formed AOT film (■). The results are compared to the adsorption isotherm obtained for Tween 20 (■), data reproduced from Figure 4.1.

The dissipation data obtained in correspondence of the adsorption data are shown in Figure 4.7. At all concentrations considered, the dissipation observed for the mixed system is larger than that for Tween 20 alone. Further, the measured dissipation for the mixed system increases as the Tween 20 concentration increases. The rate of increase in the different regions follow the qualitative trend discussed for the amount adsorbed. At high Tween 20 concentrations (above its CMC), the dissipation results obtained for the mixed system are higher than those obtained for the mixed system prepared in the reversed order (AOT added to a Tween 20 film, data in Figure 4.5), and are very similar, when statistical uncertainty is considered, to those obtained for AOT alone. In other words, the adsorbed amount for the mixed system at high Tween 20 concentration corresponds to that of Tween 20 alone, while the dissipation replicates that of AOT alone. The conclusion for both procedures (adding AOT to a Tween 20 film or, vice versa, adding Tween 20 to an AOT film) yield an adsorbed film containing both AOT and Tween 20.

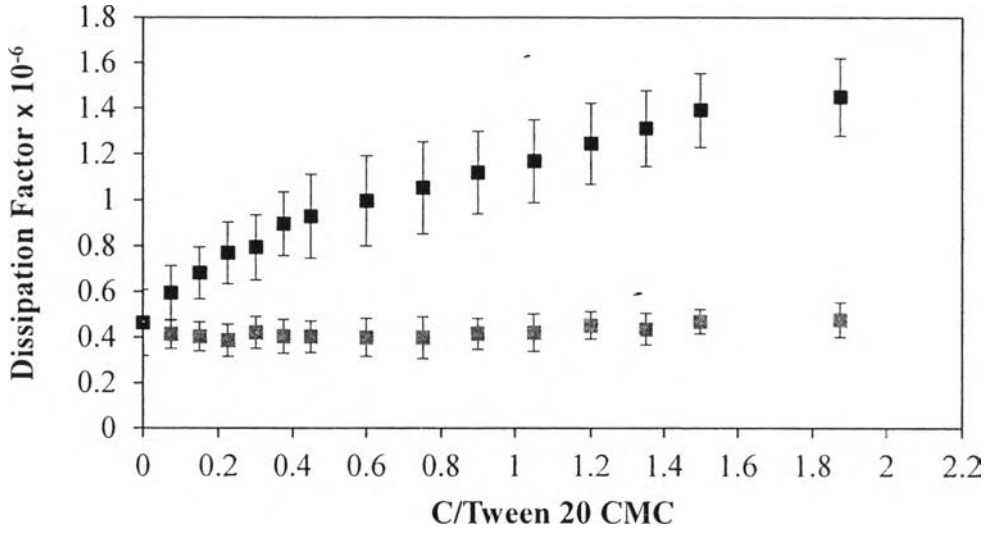

Figure 4.7 Measured energy dissipation for Tween 20 (■) and Tween 20 precovered with AOT (■) on gold surface as a function of bulk concentration corresponding to the adsorption isotherm in Figure 4.4. The results are compared to the dissipation obtained for Tween 20 (■), data reproduced from Figure 4.2.

4.3 Discussion for the Mixed Systems

Because the Tween 20 concentration in the supernatant was maintained at 1.4 its CMC during the experiments of Figures 4.4 and 4.5 while the AOT concentration was varied, and because the AOT concentration in the supernatant was maintained at 1.4 its CMC during the experiments of Figures 4.6 and 4.7 while the Tween 20 concentration was varied, the results obtained at 1.4 AOT CMC in Figures 4.4 and 4.5 and those obtained at 1.4 Tween 20 CMC in Figures 4.6 and 4.7 were obtained at the same conditions. The correspondent adsorbed mass (compare Figure 4.4 to Figure 4.6) are similar in the two procedures (when errors are accounted for), while the film dissipations differ (compare Figure 4.5 to Figure 4.7). This suggests that the films obtained during the experiments are not representative of equilibrated systems. This observation is not the only instance of non-equilibrium behavior; namely mass adsorbed for pure AOT in Figure 4.6 (concentration equals zero on this plot; does not match the value shown for AOT concentration = 1.4(CMC) in Figure 4.1. A similar statement holds for the dissipations of pure AOT at the same concentration in Figure 4.7 and Figure 4.2 respectively. The values in Figures 4.6 and 4.7 were measured after changing the concentration from 0 to 1.4(CMC) respectively, while that in Figures 4.1 and 4.2 were determined by stepping the concentrations over small increments until 1.4(CMC) was reached. None of this non-equilibrium behavior was found for Tween 20 however. In the previous paper (Gutig *et al.*, 2008), the authors also found that the amount adsorbed when adsorption occurred from a bulk concentration above the CMC is much less than that from increasing the surfactant concentrations in a series of steps but in this case the surfactant was nominally a single component. The results in this work is not the only one to report such behavior; Atkin *et al.* (2003) reported that different adsorbed amounts were obtained if adsorption was allowed to occur in an increasing step-by-step fashion or a decreasing step-by-step fashion. Certain surfactant mixtures and impure surfactants might take many hours or days to reach constant surface tensions. Perhaps these experiments indicate that equilibrium takes a very long time on a solid surface as well as at the air-liquid interface when the amount of surfactant adsorbed on a solid surface is small compared to the amount of surfactant in solution.

4.4 Dynamics of Adsorption

The time required for adsorption was also measured. In the previous paper (Gutig *et al.*, 2008), they found rate constants by fitting adsorption models with either one-step rate (Equation 4.1) or two-step rate models (Equation 4.2) (Biswas and Chattoraj, 1998). A two-step model was necessary to adequately fit the data here as well. The rate constants obtained for AOT and Tween 20 are shown in Table 4.3.

One-step rate model : $$q_t = q_o + k_o t \quad (4.1)$$

Two-step rate model : $$q_t = q_e - A_1 e^{-k_1 t} - A_2 e^{-k_2 t} \quad (4.2)$$

Table 4.3 Parameters from Fitting the Adsorption Data on Gold to Kinetics Models

Rate	[AOT]		[Tween 20]	
constant	0 → 0.1(CMC)	0 →1.4(CMC)	0 →0.1(CMC)	0 →1.4(CMC)
k_1 (min^{-1})	0.157 ± 0.01	0.216 ± 0.01	0.128 ± 0.01	1.446 ± 0.04
k_2 (min^{-1})	0.016 ± 0.003	0.006 ± 0.0003	0.041 ± 0.01	0.108 ± 0.03

Kinetic measurements with surfactant concentration below and above the CMC were performed to understand the mechanism of surfactant adsorption. The results are shown Figure 4.8. Adsorption was not detected from 0 to 150 second after injecting the surfactant solution because of the time necessary for the fluid to flow through the tubing. Overall, AOT adsorption took a longer time than Tween 20 to reach an approximately constant value (4 hours vs. less than one hour). Under identical conditions CTAB adsorption was complete within 1.5 hours (Gutig *et al.*, 2008). Overall, the rate of Tween 20 adsorption overall is similar to that of most other surfactants measured using QCM. The peak in adsorption at an intermediate time (750 seconds) for Tween 20 at 1.4(CMC) is almost certainly due to the presence of multiple components, since for a single component system a peak should not occur.

For both AOT and Tween 20 as well as CTAB (Pagac *et al.*, 1998; Atkin *et al.*, 2000; Paria and Khilar, 2004; Howard and Craig, 2009; Woods *et al.*, 2011), the initial adsorption rate (less than 300 seconds) depends on bulk surfactant concentration, with higher concentrations leading to faster adsorption, although the rate was much faster for Tween 20. It is likely that for Tween 20, micelles have a much more important role to play than for the other surfactants considered. Such an explanation has been advanced by Atkin *et al.* (2000), who also reported an increase in adsorption rate at the CMC for CTAB on silica. However, in this paper the authors concluded that monomers not micelles are adsorbing; the micelles are serving as a source of monomers. Specifically, the delocalized counterions associated with micelles enable micelles to more effectively penetrate the double layer than monomer alone due to the reduced charge per monomer that was in micelle and monomers then migrate from micelles to the surface (Atkin *et al.*, 2000). Such an explanation cannot explain the behavior of Tween 20 since this surfactant is non-ionic.

Different mechanisms have been proposed for long equilibration times (Atkin *et al.*, 2000; Atkin *et al.*, 2001). They found that CTAB adsorption on silica at 0.6 mM (0.67(CMC)) took up to 3.5 hours to reach the equilibrium and this concentration was found to have time constants much larger than other concentrations. The authors explained this long time as being due to structural rearrangements at the surface. In addition, they also observed the slow adsorption region of cetylpyridinium bromide (CPBr) from 0.274 mM (0.3(CMC)) to 0.306 mM (0.34(CMC)) on silica. For AOT, adsorption was slow for both 0.1(CMC) and 1.4(CMC) suggesting that a specific morphological structure is not responsible for slow adsorption. Another possibility for the slow kinetics is that the impurities in AOT solution might cause slow adsorption since fast-adsorbing impurities may be de-adsorbing to allow slow-adsorbing species to adsorb because these species are energetically preferred at the surface.

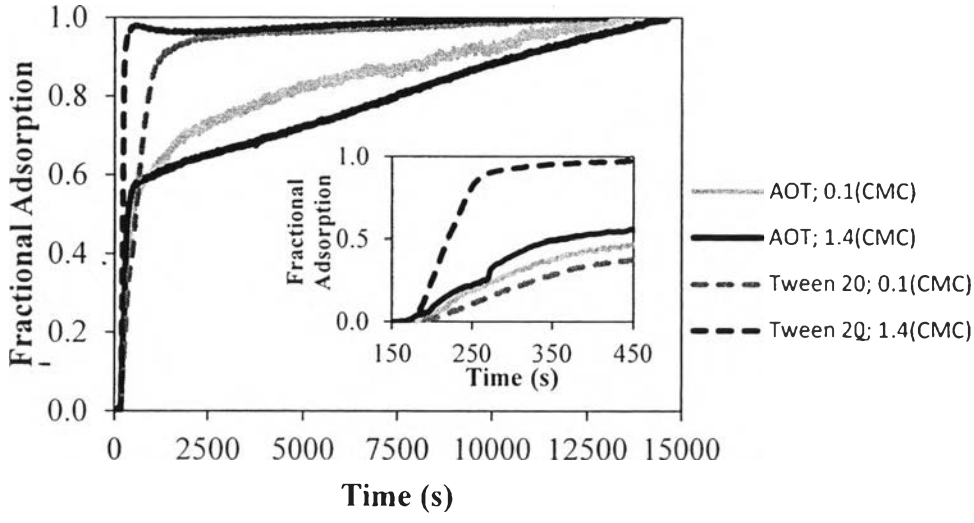

Figure 4.8 Fractional adsorption for AOT and Tween 20 as a function of time on gold surface.